Published online 12 January 2012 *Nucleic Acids Research, 2012, Vol. 40, No. 9* ***4229–4236***
doi:10.1093/nar/gkr1310

Kinetics and mechanism of G-quadruplex formation and conformational switch in a G-quadruplex of PS2.M induced by Pb^{2+}

Wei Liu[1,2,3], Hong Zhu[1], Bin Zheng[1,2,3], Sheng Cheng[1,2,3], Yan Fu[4], Wei Li[5], Tai-Chu Lau[2,3] and Haojun Liang[1,2,*]

[1]CAS Key Laboratory of Soft Matter Chemistry, Hefei National Laboratory for Physical Sciences at the Microscale, University of Science and Technology of China, Hefei, Anhui 230026, [2]Advanced Laboratory for Environmental Research and Technology (ALERT), Joint Advanced Research Center, USTC-CityU, Suzhou, Jiangsu 215124, [3]Department of Biology and Chemistry, City University of Hong Kong, Tat Chee Avenue, Kowloon, Hong Kong, [4]Key Laboratory of Systems Bioengineering, Ministry of Education, School of Chemical Engineering and Technology, Tianjin University, Tianjin 300072 and [5]Key Laboratory for Green Chemical Technology, Ministry of Education, School of Chemical Engineering and Technology, Tianjin University, Tianjin 300072, P. R. China

Received November 23, 2011; Revised December 19, 2011; Accepted December 21, 2011

ABSTRACT

DNA sequences with guanine repeats can form G-quartets that adopt G-quadruplex structures in the presence of specific metal ions. Using circular dichroism (CD) and ultraviolet-visible (UV–Vis) spectroscopy, we determined the spectral characteristics and the overall conformation of a G-quadruplex of PS2.M with an oligonucleotide sequence, $d(GTG_3TAG_3CG_3TTG_2)$. UV-melting curves demonstrate that the Pb^{2+}-induced G-quadruplex formed unimolecularly and the highest melting temperature (T_m) is 72°C. The analysis of the UV titration results reveals that the binding stoichiometry of Pb^{2+} ions to PS2.M is two, suggesting that the Pb^{2+} ions coordinate between adjacent G-quartets. Binding of ions to G-rich DNA is a complex multiple-pathway process, which is strongly affected by the type of the cations. Kinetic studies suggest that the Pb^{2+}-induced folding of PS2.M to G-quadruplex probably proceeds through a three-step pathway involving two intermediates. Structural transition occurs after adding $Pb(NO_3)_2$ to the Na^+- or K^+-induced G-quadruplexes, which may be attributed to the replacement of Na^+ or K^+ by Pb^{2+} ions and the generation of a more compact Pb^{2+}–PS2.M structure. Comparison of the relaxation times shows that the $Na^+ \rightarrow Pb^{2+}$ exchange is more facile than the $K^+ \rightarrow Pb^{2+}$ exchange process, and the mechanisms for these processes are proposed.

INTRODUCTION

G-quadruplex, a highly studied DNA motif that consists of stacks of two or more square planar arrays of four Hoogsteen hydrogen-bonded guanines called G-quartets, was first identified by Davis *et al.* (1). Interests in G-quadruplexes have been stimulated by their potential roles in a variety of cellular processes, and recently they have been considered as novel targets for drug therapy in aging and anticancer research (2–7). In addition, the G-quadruplex is a promising nanotechnology material because of its polymorphic nature (8–13). Thus, the regulation of the structural polymorphism of G-quadruplex can demonstrate a novel methodology for controlling biological processes, and for designing functional nanomaterials related to the G-quadruplexes (9).

A variety of metal ions can stabilize or switch the structures of G-quadruplexes (14,15). The most effective ions for inducing G-quadruplex formation include K^+, Na^+ and Pb^{2+} ions (16–20). The difference in the ability of these cations to bind nucleic acids and induce G-quadruplex formation can be ascribed to the difference in their sizes and their possible locations in the center of the stacks of the G-quartets. Na^+ ion is small enough to fit in the central cavity, but K^+ and Pb^{2+} ions are too large and must be located between the G-quartets planes, as confirmed by X-ray structures (19,21). Unusually, Pb^{2+} ions

*To whom correspondence should be addressed. Tel: +86 551 3607824; Fax: +86 551 3601592; Email: hjliang@ustc.edu.cn

at micromolar concentrations strongly bind with the thrombin-binding aptamer (TBA), inducing a unimolecular folded G-quadruplex (17,22,23). This highly specific metal ion binding is relatively rare for nucleic acids and provides opportunities for studies that cannot be easily done when large excess of metal ions are present, as is usually the case for monovalent cations. Interaction of Pb^{2+} ions with genetic materials may contribute to its damaging effects in human, and it is conceivable that lead's genetoxicity may arise from its ability to stabilize folded DNA structures (24–26).

Among the various G-quadruplexes being investigated, PS2.M is of particular interest, because it shows enhanced peroxidase activity when complexed with hemin (27). Travascio *et al*. (28) proposed that PS2.M folds unimolecularly into an unusual G-quadruplex with two single-base loops and two 2-base loops, and with the two terminal guanines situated in adjacent quartets. Shafer *et al*. (29) reported that K^+-induced PS2.M forms an antiparallel quadruplex at first, but is then transformed into a parallel, multistranded quadruplex with additional time, or with higher initial strand concentration. However, Sen *et al*. (30,31) proposed that PS2.M folds into a unimolecular G-quadruplex in the presence of K^+ ions. Herein, we utilized UV and CD spectroscopy to monitor the formation of the G-quadruplex of PS2.M. The binding stoichiometries of the cation–DNA complexes were determined by spectrophotometric titration. Thermal denaturation experiments were performed to investigate the stability of the G-quadruplexes. Kinetic studies were also carried out in order to provide insight into the potential pathway for the formation of the G-quadruplex as well as the folding intermediates. Pb^{2+} ions are found to be potent not only in assembling the G-quadruplex structure, but also in inducing conformational switch by displacing Na^+ or K^+ from their binding sites.

MATERIALS AND METHODS

Chemicals and reagents

The G-rich oligonucleotide, 2-(*N*-morpholino) ethanesulfonic acid (MES) and tris(hydroxymethyl) aminomethane (tris) were purchased from Shanghai Sangon Biological Engineering Technology and Services Co., Ltd. (China). All nitrate salts were of analytical grade and used without further purification. The oligomer samples were dissolved in a buffer solution consisting of 10 mM MES/Tris at pH 6.1. The oligomer solutions were then heated in a dry bath until 95°C (ABSON, USA), equilibrated for 15 min at this temperature and then slowly cooled to room temperature. The concentration of single-strand PS2.M was determined at 260 nm using a UV/Vis spectrophotometry, using a molar extinction coefficient of $184.3\,mM^{-1}\,cm^{-1}$ (32).

Circular dichroism

CD spectra were obtained using a JASCO J-810 spectropolarimeter at 25°C, which was maintained by a Julabo temperature controller. The final oligomer concentrations were in the range of 15–25 μM. Each measurement was recorded from 220 to 350 nm at a scanning rate of $100\,nm\,min^{-1}$ using a sealed 1-mm path length quartz cuvette. The spectra were collected with a response time of 0.1 s and data intervals of 0.2 nm. The final spectra were the averages of three measurements. The scan of the buffer alone under the same condition was used as the blank, and subtracted from the average scan for each sample. The cell holding chamber was flushed with a constant stream of dry nitrogen gas to avoid water condensation on the cell exterior.

UV–Vis absorption titration experiments

The extent of the PS2.M folding was evaluated by measuring UV absorbance changes at 303 nm as a function of the concentration of added $Pb(NO_3)_2$. These experiments are required prior to the kinetic experiments, not only to establish the expected changes in absorption, but also to determine the minimum concentration of $Pb(NO_3)_2$ necessary for inducing a complete folding. UV absorption spectra were measured at 1-nm intervals from 220 to 350 nm using a Shimadzu 1800 spectrophotometer (Shimadzu, Japan) equipped with a digital circulating water bath maintained at 25°C. Equal volumes of $Pb(NO_3)_2$ and oligomer in the same buffer were mixed in a sealed tandem cuvette with a path length of 10 mm. The oligomer concentration before and after mixing was 5.0 and 2.5 μM, respectively. After each addition of $Pb(NO_3)_2$, the difference spectra $\Delta A^{\lambda} = A^{\lambda}_{U} - A^{\lambda}_{F}$ were obtained by subtracting the absorption spectrum from the spectrum of the fully unfolded oligonucleotide. The resulting titration data ($\Delta\varepsilon$), were then plotted as a function of the concentration of $Pb(NO_3)_2$.

Thermal denaturation experiments

Nucleic acid structures are sensitive to temperature. Hence, UV-melting profiles can be used to determine the melting temperature (T_m) of the cation-induced G-quadruplexes and the temperature range in which the complexes can be stable. In a typical experiment, the melting curve was obtained by monitoring the UV absorbance, at either 295 nm (for Na^+ and K^+ systems) or 303 nm (for Pb^{2+} system), as a function of temperature using a sealed 10 mm path-length quartz cell. The samples were first held at 15°C for 5 min and then heated to 95°C with a heating rate of $0.2°C\,min^{-1}$. The T_m values of the complexes were calculated by fitting the experimental curves with a Sigma plot (33), where T_m is the midpoint temperature of the order-disorder transition of the complex.

Stopped-flow kinetic experiments

The kinetic experiments of the Pb^{2+}-induced oligomer folding process were performed by monitoring the absorbance changes using an Applied Photophysics SX–20 stopped-flow spectrophotometer. Before measurement, the oligomer samples were thermally treated as described above and incubated at the desired temperature for several minutes. Absorption spectra were collected from 250 to 350 nm with 4000 time points. To avoid low signal-to-noise ratio at the shorter wavelengths and the dead-time points, we discarded the data points collected at

wavelengths <270 nm and data before dead time prior to analysis (34). A circulating water bath was used to maintain a constant reaction temperature. The kinetic experiments were performed under pseudo-first-order conditions with the concentrations of $Pb(NO_3)_2$ at least in 10-fold excess of that of the oligomer. At least five successive mixing experiments were performed, and the results were averaged for analysis. Control experiments consisting of mixing oligomer with cation-free buffer were also performed. Kinetics of the conformational switches were conducted by adding $Pb(NO_3)_2$ into the systems containing G-quadruplexes induced by Na^+ or K^+ ions. Single–wavelength progress curves were analyzed by non-linear least-squares using single or multiple exponentials [Equation (1)] to determine the rate constants for the formation of G-quadruplex:

$$A_{t,\lambda} = A_{1,\lambda} \times \exp(-t/\tau_1) + A_{2,\lambda} \times \exp(-t/\tau_2) + A_3, \lambda \times \exp(-t/\tau_3) + A_0, \lambda \quad (1)$$

where $A_{t,\lambda}$ is the value of the absorbance at time t, $A_{0,\lambda}$ is the initial value of absorbance, $A_{1,\lambda}$, $A_{2,\lambda}$ and $A_{3,\lambda}$ are the amplitude factors for the first, second and third exponentials at wavelength λ, respectively. τ_1, τ_2 and τ_3 are the relaxation times.

RESULTS AND DISCUSSION

CD spectroscopy

CD is a technique that is quite sensitive to the conformation of anisotropic molecules and chiral super assemblies, and has been used extensively in the study of nucleic acids and G-quadruplex structures. Figure 1 shows the CD spectra of 25 μM PS2.M in the presence of different metal cations. The addition of 0.5 mM $NaNO_3$ shows little effect on the structure of PS2.M. In the presence of K^+ ions, the spectrum of PS2.M shows a positive CD peak near 295 nm, characteristic of antiparallel structure (35). Upon the addition of $Pb(NO_3)_2$, the wavelength at maximum CD intensity is shifted by almost 20 to 312 nm, and the peak minimum is located at 263 nm, indicating the Pb^{2+}-induced antiparallel G-quadruplex structure (17,23,29,36). The spectrum does not vary with time or oligomer concentration from 1 to 25 μM. This result indicates that there was no transformation to parallel folds at such low concentrations, consistent with the previous study (37). Moreover, after the G-quadruplex was formed in the presence of Pb^{2+} ions, there were no conformational changes observed upon the addition of $NaNO_3$ or KNO_3 at room temperature. On the other hand, spectral changes of PS2.M occur upon the addition of $Pb(NO_3)_2$ into the systems containing Na^+ or K^+ ions. In addition, the CD intensity of the Pb^{2+}-induced G-quadruplex is about three and six times higher than those of induced by K^+ and Na^+, respectively. These results strongly suggest that there are structural differences between G-quadruplexes induced by Na^+, K^+ and Pb^{2+} ions. Previous studies (22,23) have demonstrated that Pb^{2+}-induced G-quadruplexes generally have shorter M–O and O–O bonds than those induced by Na^+ or K^+ ions. Such compact structures are the result of the unusually high efficiency of Pb^{2+} ions in stabilizing G-quadruplexes (17,22). The increase in intensity and location shift of the CD spectrum of Pb^{2+}-induced G-quadruplex reveals a change in the dimensions of the G8 cage dimension, which corresponds with the decrease in the cage size as observed in the X-ray crystal structure (22). The overall difference in the CD spectra of the G-quadruplex in the presence of various cations may be attributed to the difference in the coordination number of cations, partial formation of G-quadruplexes with some cations and/or overall tightness of each G-quadruplex.

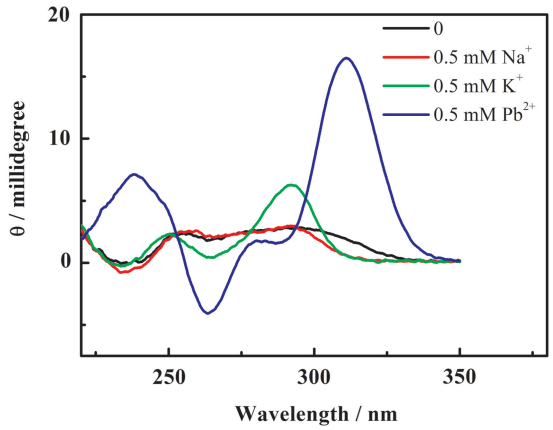

Figure 1. CD spectra of the cation-induced G-quadruplexes of PS2.M in the presence of various cations in the buffer (10 mM MES/Tris, pH 6.1) at 25°C. Concentrations of oligonucleotide were 25 μM after mixing.

Folding equilibrium titration

Previous studies have shown that the UV absorption spectrum of the Pb^{2+}-driven folded G-quadruplex possesses an absorption maximum at ~303 nm, which is distinctly different from that of the unfolded oligonucleotide (15,23). To monitor the expected absorbance change and cation binding number, we titrated PS2.M with $Pb(NO_3)_2$ at micromolar concentrations at 25°C. The absorbance changes at 303 nm were monitored as a function of the molar ratio of the cation to the oligomer and the results are shown in Figure 2. The difference spectrum $\Delta\varepsilon = \varepsilon^{\lambda}_{U} - \varepsilon^{\lambda}_{F}$ was obtained by subtracting the absorption spectrum from the spectrum of the fully unfolded oligomer. As indicated in Figure 2a, the absorbance at 303 nm increases with increasing concentration of $Pb(NO_3)_2$, which is accompanied by relatively smaller absorbance decrease in absorbance at ~245 and ~275 nm. Figure 2b shows the plot of absorbance change at 303 nm versus the $[Pb^{2+}]/[PS2.M]$ molar ratio. The result is consistent with the binding stoichiometry of two Pb^{2+} ions per oligonucleotide, which can coordinate a Pb^{2+} ion between each of the three quartets. This is contrast to a previous suggestion that only one Pb^{2+} ion binds to one oligonucleotide (29). The ability of Pb^{2+} ions to stabilize G-quadruplexes at micromolar concentrations indicates the high affinity of the Pb^{2+} ions for the DNA. Moreover, no spectral changes were observed changes

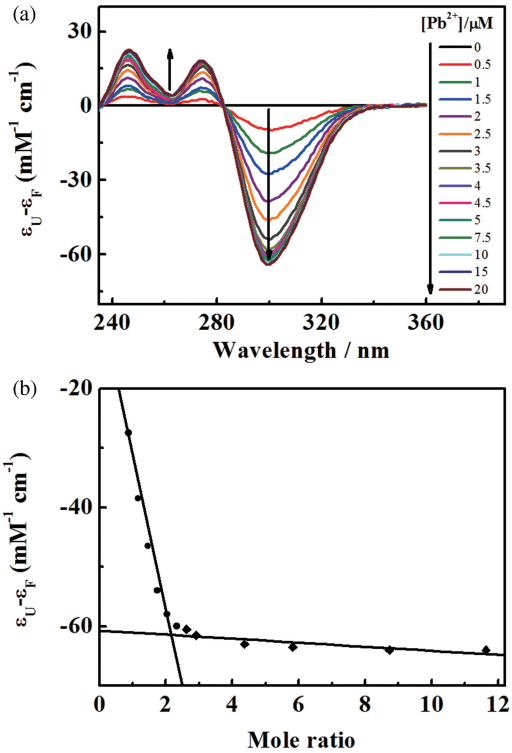

Figure 2. Spectrophotometric titration of PS2.M (2.5 μM) with of $Pb(NO_3)_2$. (**a**) Spectral changes in the titration process. The final cation concentrations after mixing are shown at the right of the panel; (**b**) Plot of absorbance change at 303 nm versus the mole ratio of $Pb(NO_3)_2$ to PS2.M. The temperature was maintained at 25°C.

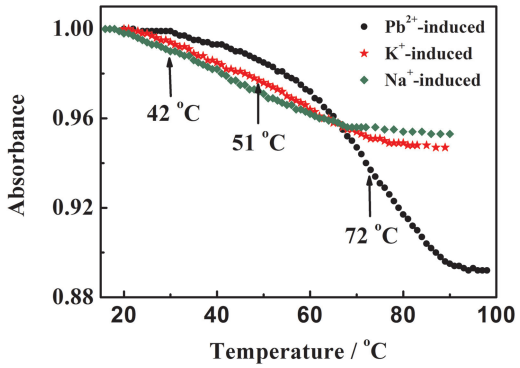

Figure 3. Denaturation profiles for the G-quadruplex of PS2.M (2.5 μM) induced by various cations in buffer solution (10 mM MES/Tris, pH 6.1). The UV-melting curves were measured at 303 nm for $Pb(NO_3)_2$ (0.5 mM) and at 295 nm for $NaNO_3$ or KNO_3 (50 mM).

when KNO_3 was added to the G-quadruplex of PS2.M induced by Pb^{2+} ions, while spectral changes occurred when $Pb(NO_3)_2$ was added to the G-quadruplex induced by K^+ ions, again indicating the high stability of Pb^{2+}–PS2.M complex. Based on these observations, the genotoxicity of Pb^{2+} ion may arise partially from its strong binding to a quadruplex formation in the genome; more closely, in the promoter regions where the quadruplexes can serve as transcription switches. Thus, if Pb^{2+} can displace K^+ from the quadruplex, but not vice versa, the switching function may be hindered, providing an explanation for genotoxicity.

Thermal denaturation profiles

UV-melting experiments were performed to examine the stability of the cation-induced G-quadruplexes (38). As shown in Figure 3, all curves demonstrate monophasic transition with different cooperativities, some broad while others somewhat sharper, depending on the ions used. The UV-melting analysis of PS2.M in the presence of 0.5 mM $Pb(NO_3)_2$ reveals a cooperative monophasic melting transition at 72 ± 2°C. Such a high-melting temperature suggests that the Pb^{2+}-induced G-quadruplex of PS2.M is stable under physiological conditions. On the other hand, in the presence of 50 mM $NaNO_3$ or KNO_3, the T_m values of the G-quadruplexes are determined to be 42 and 51°C, respectively. The low-melting temperature for the Na^+-induced G-quadruplex indicates that the complex should be largely unfolded at the physiological temperature. The higher T_m for the G-quadruplex induced by $Pb(NO_3)_2$ than those of $NaNO_3$ or KNO_3 is consistent with the higher binding affinity of the Pb^{2+} ions. In addition, the T_m remains constant over a 10-fold increase in strand concentration, indicating that the G-quadruplex is formed intramolecularly. UV-melting experiments have been previously reported (29,39,40), but the T_m values were different because different metal concentrations were used

Stopped-flow kinetic studies

Spectrophotometric changes of Pb^{2+}-induced folding of PS2.M. To our knowledge, there are few kinetic studies on the formation pathways of G-quadruplexes (41). Considering that the time scale of the folding of G-quadruplex is very short, we used stopped-flow mixing technique to acquire the spectrophotometric changes that accompany the Pb^{2+}-driven G-quadruplex formation. Figure 4 shows representative 3D plots of the wavelength and time dependence of the UV difference spectra $\Delta A^{\lambda} = A^{\lambda}_{U} - A^{\lambda}_{F}$ for the folding process of ~2.5 μM of the oligonucleotide induced by 10 μM of $Pb(NO_3)_2$. Spectra were obtained by rapid mixing at 0.1 s intervals and the folding process was completed within 5 s. The growth of a negative peak at around 303 nm indicates the formation of the Pb^{2+}-induced G-quadruplex. Analysis of the repetitive scanning spectra shows an initial rapid step with slight absorbance change at 0.03 s after mixing, this is followed by slower steps with larger absorbance changes.

Time-tracing curves of the Pb^{2+}-induced formation of G-quadruplex. The time-tracing curves of the folding process were obtained by monitoring absorbance changes at 303 nm, the maximum signal of the spectrum of the Pb^{2+}-induced G-quadruplex. In the presence of at least 10-fold excess of $Pb(NO_3)_2$, curve fitting analysis shows that three sequential first-order processes (modeling the U→I1→I2→F reaction pathway) are required to adequately reproduce the data sets for the folding of PS2.M (Figure 5). Fitting to single and

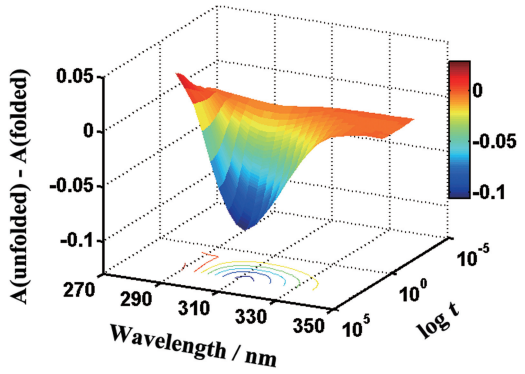

Figure 4. Representative 3D plots of the wavelength and time dependence of spectrophotometric changes accompanying the Pb^{2+}-induced folding of PS2.M. $Pb(NO_3)_2$ (20 μM) was mixed with PS2.M (5.0 μM) in buffer solution (10 mM MES/Tris, pH 6.1). The temperature was kept at 25°C.

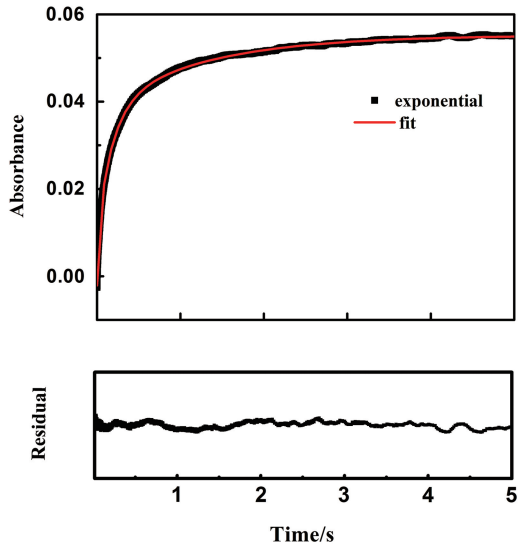

Figure 5. Representative absorbance (303 nm)/time trace of the folding of PS2.M (2.5 μM) induced by $Pb(NO_3)_2$ (0.2 mM). All measurements were performed in a buffer containing 10 mM MES/Tris (pH 6.1) at 25°C. The red line shows the non-linear least-squares fit of the data set to three exponentials. The optimized relaxation times are $\tau_1 = 0.029 \pm 0.0005$ s, $\tau_2 = 0.19 \pm 0.003$ s and $\tau_3 = 1.25 \pm 0.03$ s. The residual plot indicates the deviation of the experimental and fitted absorbance changes.

double exponential rate expressions result in large systematic deviations between the fitted and experimental progress curves. Kinetic and static difference spectra are in reasonable agreement, indicating that the kinetics account for the expected absorbance change. The residual plot shows that the three exponential function fits the experimental curve very well. A set of five curves were analyzed, and the optimal relaxation times are 0.029 ± 0.0005, 0.19 ± 0.003, 1.25 ± 0.03 s. Previous studies showed that the binding of a monovalent cation to G-quadruplex occurs on a millisecond time scale (42,43), hence in this case the first step can be interpreted as a cation binding step, which may be accompanied by partial folding of the oligonucleotide. The second step is proposed to be the folding of the PS2.M chain to give a metastable G-quadruplex, which then rearranges in the third step to give the final folded structure of the G-quadruplex. These relaxation times are much shorter than those of the G-quadruplexes induced by monovalent cations (34,44), which may be partly due to the higher charge of the Pb^{2+} ions. As expected, the folding rates are independent of the concentration of $Pb(NO_3)_2$, suggesting rate-saturation kinetics, which is in accordance with the high stability of the Pb^{2+}-induced G-quadruplex (45). Recently, a simulation study (46) on the binding of cations to G-rich DNA showed that it is a complex multiple pathway process, which is strongly affected by the type of the cations. In the present case, the proposed mechanism requires at least two intermediates for the Pb^{2+}-induced folding of a G-quadruplex of PS2.M, as shown in Equation 2 below:

$$(\text{PS2.M})_{\text{U}} + n\,\text{Pb}^{2+} \rightleftharpoons (\text{I1} - \text{Pb}^{2+}) \rightarrow \text{I2} \rightarrow (\text{PS2.M} - \text{Pb}^{2+})_{\text{F}} \quad (2)$$

where $(PS2.M)_U$ and $(PS2.M–Pb^{2+})_F$ indicate the unfolded and folded structures of PS2.M, respectively. I1 and I2 refer to the two intermediates.

Kinetic analysis of Pb^{2+} induced conformational switch of Na^+ and K^+-PS2.M complexes. Na^+ and K^+ ions are the major intracellular metal cations, which are also able to induce folding of G-quadruplex. We find that Pb^{2+} ions can not only assemble G-rich DNA segments into a G-quadruplex, but also 'switch' quadruplex structures by readily displacing K^+ or Na^+ ions from the quadruplexes. To determine whether the effect of Pb^{2+} ions on the structural rearrangement is synergetic or competitive, we investigated the conformational switches in the G-quadruplexes of PS2.M induced by Na^+ or K^+ ions in the presence of Pb^{2+} ions. Figure 6 shows the progress curves for the $Na^+ \rightarrow Pb^{2+}$ and $K^+ \rightarrow Pb^{2+}$ exchanges measured using UV stopped-flow spectrophotometry at 303 nm. A slight increase in ΔA was observed after the addition of $Pb(NO_3)_2$, and the distinctly different spectra reveal that Pb^{2+} ions 'switch' further structural transitions of the Na^+- or K^+-induced G-quadruplex.

In the case of Na^+ ions, ΔA increases from 0.05 to 0.09 for the Na^+/Pb^{2+} exchange, which may be attributed to the tighter G-quadruplex structure. The time-tracing curves were fitted to a three-exponential function, and the relaxation times are $\tau_1 = 0.0037 \pm 0.0001$ s, $\tau_2 = 0.15 \pm 0.001$ s and $\tau_3 = 2.1 \pm 0.01$ s after adding $Pb(NO_3)_2$ to the Na^+-induced G-quadruplex. Previous studies showed that the monovalent cation binding to the G-quadruplex was very fast (the relaxation time was in the order of milliseconds) (34,35), so τ_1 is assigned to the binding time of Pb^{2+} ions to the G-quadruplex. τ_2 and τ_3 are attributed to the displacement of Na^+ ions and rearrangement of the G-quadruplex, respectively, which is consistent with simulation results (46,47). Notably τ_1 for $Na^+ \rightarrow Pb^{2+}$ switch is much shorter than that for folding of PS2.M by Pb^{2+}, which may be attributed to less conformational change in the former process. It also suggest that

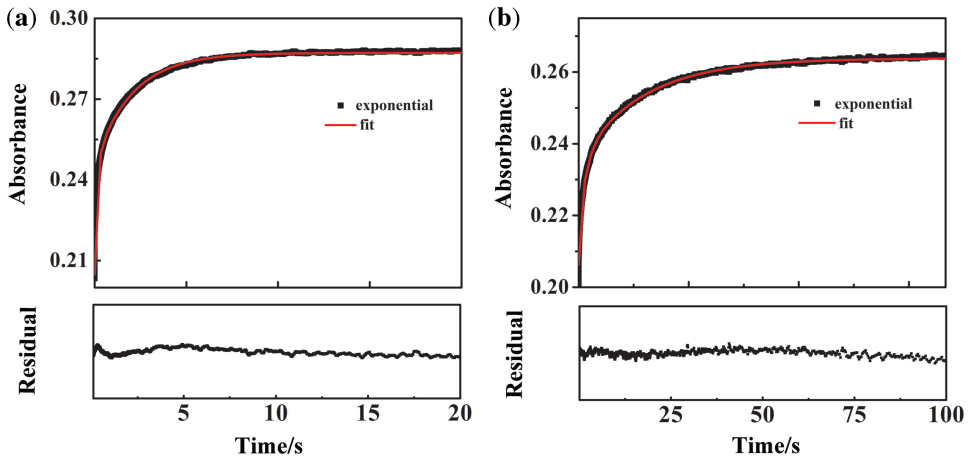

Figure 6. Time-tracing curves of conformational changes by measuring absorbance change at 303 nm for (**a**) Na^+/Pb^{2+} and (**b**) K^+/Pb^{2+} exchanges. PS2.M (5 μM) was annealed in the buffer (10 mM/Tris, pH 6.1) containing 50 mM of Na^+ or K^+ and then mixed with $Pb(NO_3)_2$ (50 μM) at 25°C. Each profile was fitted to a three-exponential function. For the Na^+/Pb^{2+} exchange, the optimized relaxation times are $\tau_1 = 0.0037 \pm 0.0001$ s, $\tau_2 = 0.15 \pm 0.001$ s and $\tau_3 = 2.1 \pm 0.01$ s. For the K^+/Pb^{2+} exchange, the optimized relaxation times are $\tau_1 = 0.23 \pm 0.007$ s, $\tau_2 = 1.88 \pm 0.03$ s and $\tau_3 = 17.6 \pm 0.2$ s. The residual plots indicate the deviation of the experimental and fitted absorbance changes.

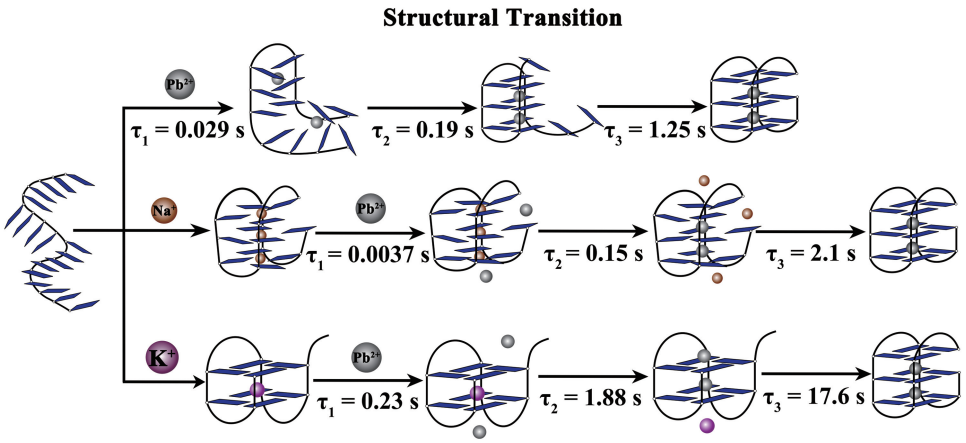

Figure 7. Proposed mechanism of the structural transition in a G-quadruplex of PS2.M induced by Pb^{2+} ions. Guanine bases are shown as rectangles.

Na^+ and Pb^{2+} ions may occupy different sites in the G-quadruplex, so there is little competition/repulsion between the ions during the binding process.

In the case of $K^+ \rightarrow Pb^{2+}$ exchange, the time-tracing curves were fitted in the same manner and the relaxation times are $\tau_1 = 0.23 \pm 0.007$ s, $\tau_2 = 1.9 \pm 0.03$ s and $\tau_3 = 17 \pm 0.2$ s after adding Pb^{2+} ions to the G-quadruplex induced by K^+ ions. Notably τ_1 for K^+ is much larger than that for Na^+ ions, which may be due to K^+ and Pb^{2+} occupying the same binding sites, hence there is electrostatic repulsion between Pb^{2+} and K^+ ions during the binding process. The second and third steps are probably due to the displacement of K^+ ions and further arrangement of the oligonucleotide to give the final Pb^{2+}-stabilized G-quadruplexes. In comparison with K^+, Pb^{2+} can form a more stable G-quadruplex structure, which is probably the reason that Pb^{2+} can induce K^+-stabilized G-quadruplex to undergo a conformational change.

Mechanism of the structural transition. Based on the kinetic and equilibrium studies, a mechanism for the formation and conformational switch of the G-quadruplex of PS2.M is proposed as shown in Figure 7. In this mechanism, two Pb^{2+} ions are required to fully assemble PS2.M with the Pb^{2+} ions coordinating between the adjacent G-quartets. Although Deng *et al*. (48) revealed that Sr^{2+} ions bond to a short RNA quadruplex in every other G-quartet region. Considering the structural difference of the two G-quadruplexes and the different properties between Pb^{2+} and Sr^{2+} ions, we think the proposed structure is the most reasonable one based on our results and data from the literature. Presumably the strong bonding between the Pb^{2+} ions and the guanine ligands helps to delocalize the positive charge and stabilize the structure. In the presence of Na^+, PS2.M folds into a metastable G-quadruplex with Na^+ ions in the plane of each G-quartet, making it easier for Pb^{2+} ions to fold

a compact G-quadruplex. On the other hand, in the presence of K^+ ions, PS2.M is transformed into a relatively stable G-quadruplex with the same binding site as the Pb^{2+} ions, making it more difficult to exchange for Pb^{2+} ions. In short, the initially added Na^+ ions have a synergetic effect with Pb^{2+} ions on the structural transition of the PS2.M chain, whereas the K^+ ions have a competitive effect on this transition. This result is quite consistent with those of the previous studies (45).

CONCLUSIONS

In the present study, we have reported the kinetics and mechanisms of the formation and structural transitions in a G-quadruplex of PS2.M. We used CD and UV spectroscopy to observe the characteristic spectra of the G-quadruplex of PS2.M in the presence of various cations. The equilibrium titrations demonstrate that, at micromolar concentrations, the Pb^{2+} binding stoichiometry is two, with the Pb^{2+} ions probably coordinating between the adjacent G-quartets. The thermal denaturation experiments show that the T_m of the Pb^{2+}–PS2.M complex is markedly higher than those of the Na^+- or K^+-induced ones, which is consistent with the high stability of the Pb^{2+}-induced G-quadruplex. Kinetic studies show that the Pb^{2+}-induced folding of PS2.M into a G-quadruplex probably proceeds through a three-step pathway with two intermediates. Pb^{2+} ions also cause structural transition of the G-quadruplex of PS2.M induced by Na^+ or K^+ ions, which may be ascribed to the exchange of Pb^{2+} with Na^+ or K^+ ions and the generation of a more compact structure. We believe that this facile structural transition in G-quadruplex would be very useful for the design of molecular switch or other functional materials.

FUNDING

Funding for open access charge: National Natural Science Foundation of China (Grant Nos. 20934004 and 91127046); NBRPC (Grant Nos. 2012CB821500 and 2010CB934500); 'Bairen' fund of CAS.

Conflict of interest statement. None declared.

REFERENCES

1. Gellert,M., Lipsett,M.N. and Davies,D.R. (1962) Helix formation by guanylic acid. *Proc. Natl Acad. Sci. USA*, **48**, 2013–2018.
2. Guschlbauer,W., Chantot,J.F. and Thiele,D. (1990) Four-stranded nucleic acid structures 25 years later: from guanosine gels to telomer DNA. *J. Biomol. Struct. Dyn.*, **8**, 491–511.
3. Jing,N.J. and Hogan,M.E. (1998) Structure-activity of tetrad-forming oligonucleotides as a potent anti-HIV therapeutic drug. *J. Biol. Chem.*, **273**, 34992–34999.
4. Mergny,J.L., Phan,A.T. and Lacroix,L. (1998) Following G-quartet formation by UV-spectroscopy. *FEBS Lett.*, **435**, 74–78.
5. Han,H.Y. and Hurley,L.H. (2000) G-quadruplex DNA: a potential target for anti-cancer drug design. *Trends Pharmacol. Sci.*, **21**, 136–142.
6. Neidle,S. and Parkinson,G. (2002) Telomere maintenance as a target for anticancer drug discovery. *Nat. Rev. Drug Discov.*, **1**, 383–393.
7. Olaussen,K.A., Dubrana,K., Dornont,J., Spano,J.P., Sabatier,L. and Soria,J.C. (2006) Telomeres and telomerase as targets for anticancer drug development. *Crit. Rev. Oncol. Hemat.*, **57**, 191–214.
8. Sugimoto,N., Toda,T. and Ohmichi,T. (1998) Reaction field for efficient porphyrin metallation catalysis produced by self-assembly of a short DNA oligonucleotide. *Chem. Commun.*, 1533–1534.
9. Sidorov,V., Kotch,F.W., El-Khouedi,M. and Davis,J.T. (2000) Toward artificial ion channels: self-assembled nanotubes from calix[4]arene-guanosine conjugates. *Chem. Commun.*, 2369–2370.
10. Willner,I., Yi,X., Pavlov,V., Gill,R. and Bourenko,T. (2004) Lighting up biochemiluminescence by the surface self-assembly of DNA-hemin complexes. *Chembiochem*, **5**, 374–379.
11. Li,D., Shlyahovsky,B., Elbaz,J. and Willner,I. (2007) Amplified analysis of low-molecular-weight substrates or proteins by the self-assembly of DNAzyme-aptamer conjugates. *J. Am. Chem. Soc.*, **129**, 5804–5805.
12. Willner,I., Cheglakov,Z., Weizmann,Y. and Sharon,E. (2008) Analysis of DNA and single-base mutations using magnetic particles for purification, amplification and DNAzyme detection. *Analyst*, **133**, 923–927.
13. Willner,I., Elbaz,J. and Shlyahovsky,B. (2008) A DNAzyme cascade for the amplified detection of Pb^{2+} ions or L-histidine. *Chem. Commun.*, 1569–1571.
14. Chen,F.M. (1992) Sr^{2+} facilitates intermolecular G-quadruplex formation of telomeric sequences. *Biochemistry*, **31**, 3769–3776.
15. Hud,N.V. and Pavec,J. (2006) The role of cations in determining quadruplex structure and stability. In: Neidle,S. and Balasubramanian,S. (eds), *Quadruplex Nucleic Acids*. RSC Publishing, Cambridge, UK, pp. 100–130.
16. Sen,D. and Gilbert,W. (1990) A sodium-potassium switch in the formation of four-stranded G4-DNA. *Nature*, **344**, 410–414.
17. Smirnov,I. and Shafer,R.H. (2000) Lead is unusually effective in sequence-specific folding of DNA. *J. Mol. Biol.*, **296**, 1–5.
18. Dai,J.X., Punchihewa,C., Ambrus,A., Chen,D., Jones,R.A. and Yang,D.Z. (2007) Structure of the intramolecular human telomeric G-quadruplex in potassium solution: a novel adenine triple formation. *Nucleic Acids Res.*, **35**, 2440–2450.
19. Engelhart,A.E., Plavec,J., Persil,O. and Hud,N.V. (2009) Metal ion interaction with G-quadruplex structures. In: Hud,N.V. (ed.), *Nucleic Acid–Metal Ion Interactions*. RSC Publishing, pp. 118–147.
20. Zhang,J.D., Dai,J.X., Veliath,E., Jones,R.A. and Yang,D.Z. (2010) Structure of a two-G-tetrad intramolecular G-quadruplex formed by a variant human telomeric sequence in K^+ solution: insights into the interconversion of human telomeric G-quadruplex structures. *Nucleic Acids Res.*, **38**, 1009–1021.
21. Kelly,J.A., Feigon,J. and Yeates,T.O. (1996) Reconciliation of the X-ray and NMR structures of the thrombin-binding aptamer d(GGTTGGTGTGGTTGG). *J. Mol. Biol.*, **256**, 417–422.
22. Kotch,F.W., Fettinger,J.C. and Davis,J.T. (2000) A lead-filled G-quadruplex: insight into the G-Quartet's selectivity for Pb^{2+} over K^+. *Org. Lett.*, **2**, 3277–3280.
23. Li,T., Wang,E.K. and Dong,S.J. (2009) Potassium-lead-switched G-quadruplexes: a new class of DNA logic gates. *J. Am. Chem. Soc.*, **131**, 15082–15083.
24. Gerber,G.B., Leonard,A. and Jacquet,P. (1980) Toxicity, mutagenicity and teratogenicity of lead. *Mutat. Res.*, **76**, 115–141.
25. Dhar,A. and Banerjee,P.K. (1983) Impact of lead on nucleic acids and incorporation of labelled amino acid into protein. *Int. J. Vitam. Nutr. Res.*, **53**, 349–354.
26. Hitzfeld,B., Planas-Bohne,F. and Taylor,D. (1989) The effect of lead on protein and DNA metabolism of normal and lead-adapted rat kidney cells in culture. *Biol. Trace Elem. Res.*, **21**, 87–95.
27. Travascio,P., Bennet,A.J., Wang,D.Y. and Sen,D. (1999) A ribozyme and a catalytic DNA with peroxidase activity: active sites versus cofactor-binding sites. *Chem Biol*, **6**, 779–787.
28. Travascio,P., Witting,P.K., Mauk,A.G. and Sen,D. (2001) The peroxidase activity of a hemin–DNA oligonucleotide complex: free radical damage to specific guanine bases of the DNA. *J. Am. Chem. Soc.*, **123**, 1337–1348.

29. Majhi,P.R. and Shafer,R.H. (2006) Characterization of an unusual folding pattern in a catalytically active guanine quadruplex structure. *Biopolymers*, **82**, 558–569.
30. Lee,H.W., Chinnapen,D.J.F. and Sen,D. (2004) Structure-function investigation of a deoxyribozyme with dual chelatase and peroxidase activities. *Pure Appl. Chem.*, **76**, 1537–1545.
31. Travascio,P., Sen,D. and Bennet,A.J. (2006) DNA and RNA enzymes with peroxidase activity - an investigation into the mechanism of action. *Can. J. Chem.*, **84**, 613–619.
32. Gray,D.M., Hung,S.H. and Johnson,K.H. (1995) Absorption and circular-dichroism spectroscopy of nucleic-acid duplexes and triplexes. *Method Enzymol.*, **246**, 19–34.
33. Hatzakis,E., Okamoto,K. and Yang,D. (2010) Thermodynamic stability and folding kinetics of the major G-quadruplex and its loop isomers formed in the nuclease hypersensitive element in the human c-Myc promoter: effect of loops and flanking segments on the stability of parallel-stranded intramolecular G-quadruplexes. *Biochemistry*, **49**, 9152–9160.
34. Gray,R.D. and Chaires,J.B. (2008) Kinetics and mechanism of K^+- and Na^+-induced folding of models of human telomeric DNA into G-quadruplex structures. *Nucleic Acids Res.*, **36**, 4191–4203.
35. Lu,M., Guo,Q. and Kallenbach,N.R. (1993) Thermodynamics of G-tetraplex formation by telomeric DNAs. *Biochemistry*, **32**, 598–601.
36. Smirnov,I.V., Kotch,F.W., Pickering,I.J., Davis,J.T. and Shafer,R.H. (2002) Pb EXAFS studies on DNA quadruplexes: identification of metal ion binding site. *Biochemistry*, **41**, 12133–12139.
37. Renčiuk,D., Kejnovská,I., Školáková,P., Bednářová,K., Motlová,J. and Vorlíčková,M. (2009) Arrangements of human telomere DNA quadruplex in physiologically relevant K^+ solutions. *Nucleic Acids Res.*, **37**, 6625–6634.
38. Lane,A.N., Chaires,J.B., Gray,R.D. and Trent,J.O. (2008) Stability and kinetics of G-quadruplex structures. *Nucleic Acids Res.*, **36**, 5482–5515.
39. Majhi,P.R., Qi,J., Tang,C.F. and Shafer,R.H. (2008) Heat capacity changes associated with guanine quadruplex formation: an isothermal titration calorimetry study. *Biopolymers*, **89**, 302–309.
40. Li,T., Wang,E.K. and Dong,S.J. (2010) Lead(II)-induced allosteric G-quadruplex DNAzyme as a colorimetric and chemiluminescence sensor for highly sensitive and selective Pb^{2+} detection. *Anal. Chem.*, **82**, 1515–1520.
41. Mergny,J.L., Gros,J., De Cian,A., Bourdoncle,A., Rosu,F., Sacca,B., Guittat,l., Amrane,S., Mills,M., Alberti,P. *et al.* (2006) Energetics, kinetics and dynamics of quadruplex folding. In: Neidle,S. and Balasubramanian,S. (eds), *Quadruplex Nucleic Acids*. RSC Publishing, Cambridge, UK, pp. 31–80.
42. Hud,N.V., Smith,F.W., Anet,F.A.L. and Feigon,J. (1996) The selectivity for K^+ versus Na^+ in DNA quadruplexes is dominated by relative free energies of hydration: a thermodynamic analysis by H-1 NMR. *Biochemistry*, **35**, 15383–15390.
43. Hud,N.V., Schultze,P., Sklenar,V. and Feigon,J. (1999) Binding sites and dynamics of ammonium ions in a telomere repeat DNA quadruplex. *J. Mol. Biol.*, **285**, 233–243.
44. Chaires,J.B., Gray,R.D. and Li,J. (2009) Energetics and kinetics of a conformational switch in G-Quadruplex DNA. *J. Phys. Chem. B*, **113**, 2676–2683.
45. Liu,W., Fu,Y., Zheng,B., Cheng,S., Li,W., Lau,T.C. and Liang,H.J. (2011) Kinetics and mechanism of conformational changes in a g-quadruplex of thrombin-binding aptamer induced by Pb^{2+}. *J. Phys. Chem. B*, **115**, 13051–13056.
46. Reshetnikov,R.V., Sponer,J., Rassokhina,O.I., Kopylov,A.M., Tsvetkov,P.O., Makarov,A.A. and Golovin,A.V. (2011) Cation binding to 15-TBA quadruplex DNA is a multiple-pathway cation-dependent process. *Nucleic Acids Res.*, **39**, 9789–9802.
47. Mashimo,T., Yagi,H., Sannohe,Y., Rajendran,A. and Sugiyama,H. (2010) Folding pathways of human telomeric type-1 and type-2 G-quadruplex structures. *J. Am. Chem. Soc.*, **132**, 14910–14918.
48. Deng,J.P., Xiong,Y. and Sundaralingam,M. (2001) X-ray analysis of an RNA tetraplex $(UGGGGU)_4$ with divalent Sr^{2+} ions at subatomic resolution (0.61 Å). *Proc. Natl Acad. Sci. USA*, **98**, 13665–13670.